Halide Perovskites

Halide perovskites (HPs), with an excellent photoactive nature, dielectric, piezoelectric, ferroelectric, and pyroelectric properties, have been potential candidates for obtaining flexible nanogenerator-based self-powered sensors including light, pressure, and temperature. Additionally, the photo-stimulated dielectric, piezoelectric, and triboelectric properties of HPs make them efficient entrants for developing bimodal and multimode sensors to sense multi-physical signals individually or simultaneously.

1. Introduction

Halide perovskite materials consist of three-dimensional ABX_3-type crystal structures (**Figure 1**, crystal structure). In ABX_3, A denotes the monovalent organic or inorganic cation (such as $MA^+ = CH_3NH_3^+$, $FA = CH(NH_2)_2^+$ and Cs^+), B represents the divalent cation (such as Pb^{2+}, Sn^{2+}, and Ge^{2+}), and X is the halide anion (Cl, Br, I). In the crystal structure, cation A is coordinated with 12 neighboring X, and cation B is connected with 6 X anions, forming cuboctahedral and octahedral geometries, respectively. The structural formability of the 3D-ABX_3 HPs and their stability were determined by the Goldschmidt tolerance factor (t) and the octahedral factors (μ) [1][2]. The tolerance factor, $t = (r_A + r_X)/\sqrt{2}(r_B + r_X)$, where r_A, r_B, and r_X represent the effective ionic radii of A, B, and X in the HP, respectively. The r_B/r_X is defined as an octahedral factor (μ) and is directly correlated with a BX_6 octahedron, playing an important role in the multifunctional properties of HP materials. The tolerance factor values for HP materials were found to be within the 0.8–1.11 range, while the octahedral factor values were in the range of 0.44–0.90 [3][4]. The calculated t values for cubic, orthorhombic, and hexagonal structured HPs were 0.8 < t < 1.0, t < 0.8, and t > 1, respectively [2][5]. Numerous methods have been proposed to fabricate HP thin films, such as the one-step solution process, two-step sequential deposition, vapor deposition method, and vapor-assisted solution process [6][7][8][9]. Solution methods have been promoted due to simple and low-temperature fabrication ways and their compliance with flexible and large-scale devices [10][11].

Furthermore, the solution methods are promising to control crystalline formation better, leading to tunable properties at nano/micro-scale [12][13]. These HP-based materials have been considered to fabricate flexible nanogenerators owing to their impressive dielectric, ferroelectric, piezoelectric, and pyroelectric properties and beneficial features such as low-temperature and large-scale fabrication routes and controllable properties [14][15][16][17][18]. In particular, the dielectric and piezoelectric properties of HP-based materials are remarkable and nearly similar to those of ceramic materials [11][13][14][19][20][21]. Generally, the dielectric material is electrically an insulator and will readily polarize under an applied electric field. The ability of a material to store electrical energy can be estimated by its dielectric permittivity (ε_r) values. However, the dielectric loss factor describes the inefficiency of a material to hold the stored energy. Consequently, a material with a high loss factor cannot hold the charge completely indicating leaky nature of the sample. Therefore, materials with larger dielectric constant values and low dissipation factor values tend to generate higher output performance in nanogenerator applications because the nanogenerators are designed as part of capacitors [20]. Many researchers have demonstrated the dielectric properties of HP-based materials and also systematically examined the changes in dielectric properties of compositionally tuned HP materials [11][13][14][21]. The dielectric polarization mechanism in HP-based materials is nearly similar to well-known ceramic perovskite materials. The existing organic cation at the center of an HP-crystal structure (e.x., MA^+ cation in $MAPbI_3$) disorders under an applied field; thus, resulting in a dipolar polarization in HPs [11].

As depicted in **Figure 2**a, the most widely used $MAPbI_3$ perovskite revealed an ε_r value of ~52 and low dissipation value of ~0.02 at an applied frequency of 100 kHz [19]. Moreover, $FAPbI_3$ perovskite exhibited an improved dielectric property due to the presence of a larger cation (FA^+) that has larger dipole momentum compared to that of MA^+ cation [22]. In addition, the dielectric properties of HPs can be significantly enhanced by partial tuning of its composition. For example, the reported halide-doped $MAPbI_3$ perovskite samples displayed a notable enhancement in dielectric properties upon halide doping (either Cl or Br) [14]. In particular $MAPbI_{3-x}Cl_x$ displayed a high ε_r value of ~90.9. The improved property is

not only because of improved grain size but also the existence of binary systems such as $MAPbI_3$ and $MAPbCl_3$ in the final film which led to interfacial polarization between two phases. Similarly, the Fe-incorporated $MAPbI_3$ unveiled enhanced ε_r value of ~107 upon partial incorporation of Fe (x = 0.07) [13]. The improved dielectric properties promoted the enhancement in piezoelectric output performance of the $MAPb_{1-x}Fe_xI_3$ based PENG. Furthermore, the lead-free Sn-based HP materials also possess high dielectric properties [23].
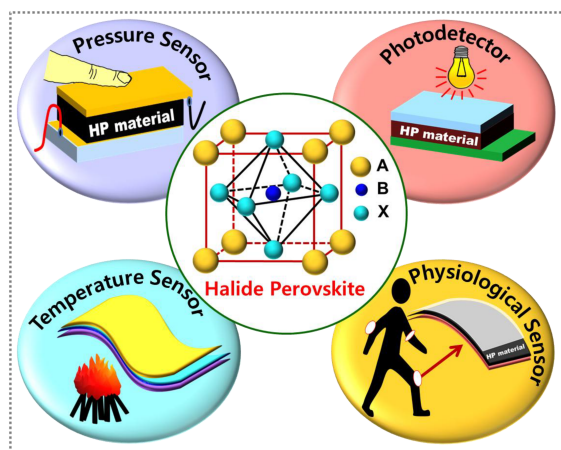
Figure 1. Schematic illustration of ABX_3-type halide perovskite structure and their utility in nanogenerator-based self-powered sensing applications.
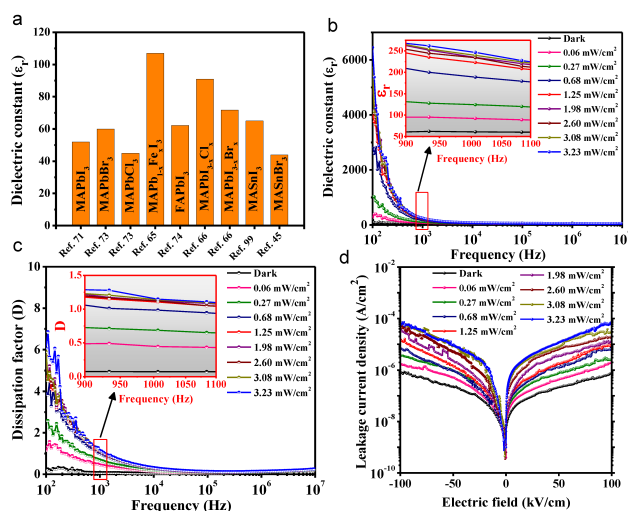
**Figure 2.** (**a**) Dielectric constants of various frequently used HP materials. Light intensity effect on frequency-dependent (**b**) dielectric constant and (**c**) dissipation factor of $MAPbI_3$-PVDF composite films. (**d**) Light intensity effect on leakage current density of $MAPbI_3$-PVDF composite films as a function of applied electric field. (**b**–**d**) Reprinted with permission from ref. [24], Copyright 2020, American Chemical Society.

2. Halide Perovskite Nanogenerator-Based Self-Powered Bimodal Sensors

Recently, several emerging sensor technologies have been developed to detect single-mode external stimuli, such as light, pressure, temperature, and humidity [25][26][27][28]. However, emerging a flexible single sensor unit capable of sensing multiple signals simultaneously is of great significance. Stacking or incorporating single-mode sensor units to build a multimode sensor can be constrained by the signal interference of different sensor units and disparities in their mechanical properties [29][30]. Therefore, it is of prodigious importance to fabricate a flexible single-structure bi/multifunctional sensor capable of perceiving various external signals using flexible materials in simple and low-cost methods. Hence, HP materials are the potential entrants to develop bi/multifunctional sensor devices in facile ways owing to the combined properties such as optoelectronic, piezo/ferroelectric, pyroelectric, and thermoelectric properties [12][19][31][32][33]. Eom et al. constructed the first HP material-based self-powered bimodal sensor (i.e., pressure cum light sensor) covering the PENG structure of glass/AAA/$MAPbI_3$/SiO_2/AAA (**Figure 3**a) (Here, AAA is AZO-Au-AZO multilayer) [34]. The $MAPbI_3$ perovskite thin film was prepared using the chemical vapor deposition (CVD) technique to study its long-term air-stability. The sputtered thin SiO_2 layer helped to prevent the electrical short-circuit of the device. The nanogenerator poled at 60 kV/cm exhibited a linearly increasing trend in piezoelectric output with increasing applied pressure from 5 to 70 kPa and obtained the pressure sensitivity value of ~8.43 mV/kPa (see **Figure 3**b). The device was simultaneously exposed to light while applying strain (30 kPa) to explore the bimodal sensing (pressure and light) features of the nanogenerator. It was observed that the device displayed a notable dependency on the intensity of focused light (**Figure 3**c), signifying the ability of the device to identify different intensities of light in a self-powered way. Another research group has also verified the multimode sensing (i.e., light and pressure signals sensing) ability of inorganic HP material-based TENG [35]. The

reported light-stimulated e-skin-based TENG has the structure of PET/PEDOT: PSS/CsPbBr$_3$/Au. It was operated based on combined photoelectric and triboelectric effects of CsPbBr$_3$ material, as illustrated in **Figure 3**d. Under repeated vertical contact-separations of the e-skin by finger tapping, the triboelectric output was notably increased with increasing applied force, indicating the low-level pressure sensing ability of the nanogenerator in a self-powered way (**Figure 3**e).

Additionally, authors have used the same device to identify the various intensities of light by illuminating the e-skin using UV-light (~365 nm) for 8 s at an applied force of 0.3 N. They observed the light-dependent responsivity of the device, as shown in **Figure 3**f. Furthermore, it is believed that the e-skin can be successfully implemented as a memristor to comprehend the human-machine interfaces in emerging artificial intelligence systems. Improving the long-term stability of HPs is imperative and remains a key challenge irrespective of their great potentiality as active sensing materials. Recently our group has found the tremendous bimodal sensing application of HP-polymer composite by emerging long-term stable single-structure device using a simple and cost-effective approach [24]. The flexible single-structure multifunctional device capable of mechanical energy scavenging and simultaneous sensing of multi-physical signals—light and pressure—was constructed using spin-coated MAPbI$_3$-PVDF composite film onto the flexible plastic substrate followed by sputtering of gold-inter digitated electrodes (gold-IDE) (**Figure 3**g). The reported nanogenerator was successfully operated as an energy harvester. Furthermore, it was simultaneously operated as a self-powered light and pressure sensors in both piezoelectric and triboelectric modes of operation owing to the combined photovoltaic and piezo/triboelectric effects of the active composite film. It was observed that the piezoelectric output of the device under a dark state increased linearly with increasing applied pressure. It displayed high output voltage of ~33.6 V at an applied pressure of 300 kPa, making the device a potential candidate to be used as a self-powered pressure sensor with excellent pressure sensitivity of 0.107 V/kPa (**Figure 3**h).
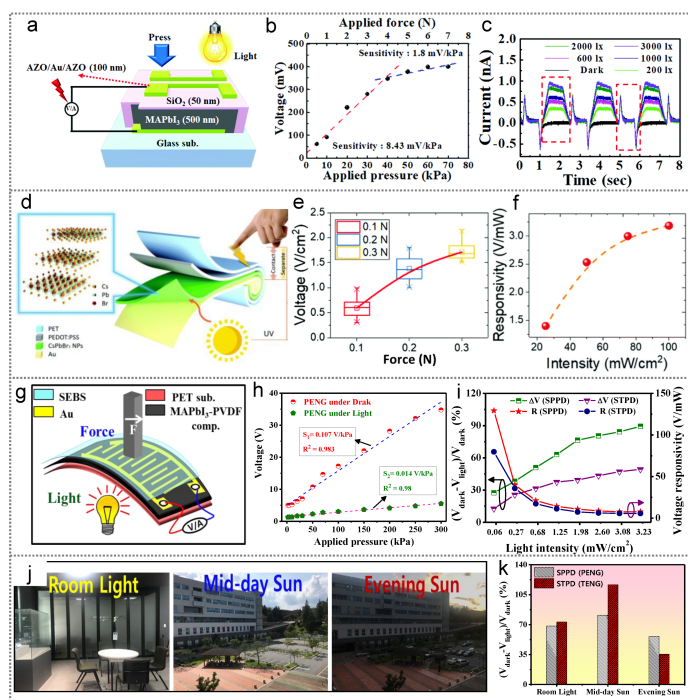
Figure 3. (**a**) Schematic illustration of MAPbI$_3$ PENG-based bimodal sensor, (**b**) corresponding pressure dependent output voltages revealing the pressure sensitivity, and (**c**) light-controlled piezoelectric output current signals at an applied constant pressure of 30 kPa. (**a**–**c**) Reprinted with permission from ref. [34], Copyright 2018, The Royal Society of Chemistry. (**d**) Schematic representation of CsPbBr$_3$ TENG-based bimodal sensor, (**e**) corresponding pressure dependent output voltage, and (**f**) responsivity of the device under various light intensities. (**d**–**f**) Reprinted with permission from ref. [35], Copyright 2021, The Royal Society of Chemistry. (**g**) Schematic sketch of MAPbI$_3$-PVDF-based bimodal sensor in PENG mode, (**h**) corresponding pressure sensitivity under dark and illumination, (**i**) corresponding voltage change and responsivity with respect to light intensities, (**j**) digital images of various light environments used for real-time operation of the device, and (**k**) corresponding change in voltages. (**g**–**k**) Reprinted with permission from ref. [24], Copyright 2020, American Chemical Society.

3. Conclusions, Outlooks, and Opportunities for Future Development

HPs have been recognized as potential entrants in numerous research fields, including solar cells, LEDs, nanogenerators, and photodetectors. Among these, the nanogenerators are the recent application of HPs. They are highly sensitive to various external perturbations, such as pressure, temperature, and light. Hence, controlling the performance of a nanogenerator under external perturbations such as temperature and pressure predominantly enabled it to be used as a self-powered temperature or pressure sensor, respectively, without dependency on a battery. Additionally, illuminating

nanogenerator significantly changes their output performance owing to the combined optoelectronic properties with piezoelectric property, or the triboelectric effect. Such light-stimulated performances of nanogenerators prominently enabled them to be used as self-powered photodetectors to detect the type of light or quantity of light intensity. This progress report briefly discussed the structural, piezoelectric, pyroelectric, and triboelectric properties of nanogenerators of HP materials. After that, we discussed the working mechanisms of several nanogenerators, including PENG, TENG, and PyENG as self-powered pressure and temperature sensors. We discussed the operation of PENG and TENG, as self-powered photodetectors under light illumination and present the possible underlying mechanisms to deliver the light-controlled outputs. Thereafter, we provided an overview of the exploration of using HP-based nanogenerators to sense various external factors such as pressure, temperature changes, and light. It is seen from the examples discussed above that when a nanogenerator is subjected to a controlled exposure to these external stimuli, continuous output voltage and current change linearly, which is a prerequisite for realizing reliable sensing systems. The recently emerging bimodal/multimodal sensing applications of HPs were also reviewed in addition to the single-mode sensor devices. We suggest the future projections of the research towards developing single-structure multimodal sensing devices.

Improving sensitivity, performance, and long-term stability of HPs is challenging despite many studies involving HPs as active sensing materials in self-powered nanogenerator-based sensors. Therefore, we identify potential directions and opportunities for future research. Recently, numerous methods, such as surface passivation, compositional tuning, fine-doping, and polymer composites, have been used to improve the air-stability of HP materials [23][24][16]. Furthermore, it has been demonstrated that the layered 2D-HPs have significantly good air and moisture stability than the 3D-HPs because of long-chain organic molecules [36][37]. Additionally, these 2D-HPs offer extremely high piezo/ferroelectric properties, helping to construct flexible, high-performance nanogenerators and reliable sensors with high sensitivity and stability [38]. Additionally, the development of eco-friendly HP material-based self-powered sensors has been highly prioritized to alleviate the environmental and human health risks. Additionally, extending the investigation to combine three or more properties may be helpful in developing trimodal/multimodal sensors to detect multiple physical signals simultaneously using a single-structure device without any signal interference. For example, our group has reported a single-structure TPS-fusion generator capable of harvesting multiple energy sources, such as thermal, mechanical, and light energies owing to the multiple properties of comprised MAPbI 3 material [39]. Finally, the flexible and stretchable self-powered sensing systems have significant potential to be for e-skin and wearable electronic device applications in the future. In this regard, considerable research should be conducted on HP materials to develop self-powered stretchable multifunctional devices that can continuously operate in harsh environs.

References

1. Goldschmidt, V.M. Krystallbau und chemische Zusammensetzung. Ber. Dtsch. Chem. Ges. 1927, 60, 1263–1296.

2. Kieslich, G.; Sun, S.; Cheetham, A.K. Solid-state principles applied to organic–inorganic perovskites: New tricks for an old dog. Chem. Sci. 2014, 5, 4712–4715.

3. Park, N.-G. Perovskite solar cells: An emerging photovoltaic technology. Mater. Today 2015, 18, 65–72.

4. Assadi, M.K.; Bakhoda, S.; Saidur, R.; Hanaei, H. Recent progress in perovskite solar cells. Renew. Sustain. Energy Rev. 2017, 81, 2812–2822.

5. Li, Z.; Yang, M.; Park, J.-S.; Wei, S.-H.; Berry, J.; Zhu, K. Stabilizing perovskite structures by tuning tolerance factor: Formation of formamidinium and cesium lead iodide solid-state alloys. Chem. Mater. 2016, 28, 284–292.

6. Wang, M.; Feng, Y.; Bian, J.; Liu, H.; Shi, Y. A comparative study of one-step and two-step approaches for MAPbI3 perovskite layer and its influence on the performance of mesoscopic perovskite solar cell. Chem. Phys. Lett. 2018, 692, 44–49.

7. Kirakosyan, A.; Kim, J.; Lee, S.W.; Swathi, I.; Yoon, S.-G.; Choi, J. Optical properties of colloidal CH3NH3PbBr3 nanocrystals by controlled growth of lateral dimension. Cryst. Growth Des. 2017, 17, 794–799.

8. Liu, M.; Johnston, M.B.; Snaith, H.J. Efficient planar heterojunction perovskite solar cells by vapour deposition. Nature 2013, 501, 395–398.

9. Chen, Q.; Zhou, H.; Hong, Z.; Luo, S.; Duan, H.-S.; Wang, H.-H.; Liu, Y.; Li, G.; Yang, Y. Planar heterojunction perovskite solar cells via vapor-assisted solution process. J. Am. Chem. Soc. 2014, 136, 622–625.

10. Wang, P.; Wu, Y.; Cai, B.; Ma, Q.; Zheng, X.; Zhang, W.-H. Solution-processable perovskite solar cells toward commercialization: Progress and challenges. Adv. Funct. Mater. 2019, 29, 1807661.

11. Jella, V.; Ippili, S.; Eom, J.-H.; Pammi, S.V.N.; Jung, J.-S.; Tran, V.-D.; Nguyen, V.H.; Kirakosyan, A.; Yun, S.; Kim, D.; et al. A comprehensive review of flexible piezoelectric generators based on organic-inorganic metal halide perovskites.

Nano Energy 2019, 57, 74–93.

12. Filip, M.R.; Eperon, G.E.; Snaith, H.J.; Giustino, F. Steric engineering of metal-halide perovskites with tunable optical band gaps. Nat. Commun. 2014, 5, 5757.

13. Ippili, S.; Jella, V.; Kim, J.; Hong, S.; Yoon, S.-G. Enhanced piezoelectric output performance via control of dielectrics in Fe2+-incorporated MAPbI3 perovskite thin films: Flexible piezoelectric generators. Nano Energy 2018, 49, 247–256.

14. Jella, V.; Ippili, S.; Yoon, S.-G. Halide (Cl/Br)-incorporated organic−inorganic metal trihalide perovskite films: Study and investigation of dielectric properties and mechanical energy harvesting performance. ACS Appl. Electron. Mater. 2020, 2, 2579–2590.

15. Park, H.; Ha, C.; Lee, J.-H. Advances in piezoelectric halide perovskites for energy harvesting applications. J. Mater. Chem. A 2020, 8, 24353–24367.

16. Jella, V.; Ippili, S.; Eom, J.-H.; Choi, J.; Yoon, S.-G. Enhanced output performance of a flexible piezoelectric energy harvester based on stable MAPbI3-PVDF composite films. Nano Energy 2018, 53, 46–56.

17. Kutes, Y.; Ye, L.; Zhou, Y.; Pang, S.; Huey, B.D.; Padture, N.P. Direct observation of ferroelectric domains in solution-processed CH3NH3PbI3 perovskite thin films. J. Phys. Chem. Lett. 2014, 5, 3335–3339.

18. Dong, Q.; Song, J.; Fang, Y.; Shao, Y.; Ducharme, S.; Huang, J. Lateral-structure single-crystal hybrid perovskite solar cells via piezoelectric poling. Adv. Mater. 2016, 28, 2816–2821.

19. Kim, Y.J.; Dang, T.V.; Choi, H.J.; Park, B.J.; Eom, J.H.; Song, H.A.; Seol, D.; Kim, Y.; Shin, S.H.; Nah, H.; et al. Piezoelectric properties of CH3NH3PbI3 perovskite thin films and their applications in piezoelectric generators. J. Mater. Chem. A 2016, 4, 756–763.

20. Ippili, S.; Jella, V.; Thomas, A.M.; Yoon, C.; Jung, J.-S.; Yoon, S.-G. ZnAl–LDH-induced electroactive β-phase and controlled dielectrics of PVDF for a high-performance triboelectric nanogenerator for humidity and pressure sensing applications. J. Mater. Chem. A 2021.

21. Yang, T.Y.; Gregori, G.; Pellet, N.; Grätzel, M.; Maier, J. The significance of ion conduction in a hybrid organic-inorganic lead-iodide-based perovskite photosensitizer. Angew. Chem. Int. Ed. 2015, 54, 7905–7910.

22. Liu, Y.; Sun, J.; Yang, Z.; Yang, D.; Ren, X.; Xu, H.; Yang, Z.; Liu, S.F. 20-mm-large single-crystalline formamidinium-perovskite wafer for mass production of integrated photodetectors. Adv. Opt. Mater. 2016, 4, 1829–1837.

23. Ippili, S.; Jella, V.; Kim, J.; Hong, S.; Yoon, S.-G. Unveiling predominant air-stable organotin bromide perovskite toward mechanical energy harvesting. ACS Appl. Mater. Interfaces 2020, 12, 16469–16480.

24. Ippili, S.; Jella, V.; Eom, S.; Hong, S.; Yoon, S.-G. Light-driven piezo- and triboelectricity in organic−inorganic metal trihalide perovskite toward mechanical energy harvesting and self-powered sensor application. ACS Appl. Mater. Interfaces 2020, 12, 50472–50483.

25. Huang, C.-B.; Witomska, S.; Aliprandi, A.; Stoeckel, M.-A.; Bonini, M.; Ciesielski, A.; Samorì, P. Molecule—Graphene hybrid materials with tunable mechanoresponse: Highly sensitive pressure sensors for health monitoring. Adv. Mater. 2019, 31, 1804600.

26. Shekhawat, G.S.; Ramachandran, S.; Sharahi, H.J.; Sarkar, S.; Hujsak, K.; Li, Y.; Hagglund, K.; Kim, S.; Aden, G.; Chand, A.; et al. Micromachined chip scale thermal sensor for thermal imaging. ACS Nano 2018, 12, 1760–1767.

27. Liu, F.; Zheng, S.; He, X.; Chaturvedi, A.; He, J.; Chow, W.L.; Mion, T.R.; Wang, X.; Zhou, J.; Fu, Q.; et al. Highly sensitive detection of polarized light using anisotropic 2D ReS2. Adv. Funct. Mater. 2016, 26, 1169–1177.

28. Chang, S.-P.; Chang, S.-J.; Lu, C.-Y.; Li, M.-J.; Hsu, C.-L.; Chiou, Y.-Z.; Hsueh, T.-J.; Chen, I.-C. A ZnO nanowire-based humidity sensor. Superlattices Microstruct. 2010, 47, 772–778.

29. Kanao, K.; Harada, S.; Yamamoto, Y.; Honda, W.; Arie, T.; Akita, S.; Takei, K. Highly selective flexible tactile strain and temperature sensors against substrate bending for an artificial skin. RSC Adv. 2015, 5, 30170–30174.

30. Engel, J.; Chen, J.; Fan, Z.; Liu, C. Polymer micromachined multimodal tactile sensors. Sens. Actuators A 2005, 117, 50–61.

31. Röhm, H.; Leonhard, T.; Hoffmann, M.J.; Colsmann, A. Ferroelectric domains in methylammonium lead iodide perovskite thin-films. Energy Environ. Sci. 2017, 10, 950–955.

32. Rakita, Y.; B-Elli, O.; Meirzadeh, E.; Kaslasi, H.; Pelea, Y.; Hodes, G.; Lubomirsky, I.; Oron, D.; Ehre, D.; Cahen, D. Tetragonal CH3NH3PbI3 is ferroelectric. Proc. Natl. Acad. Sci. USA 2017, 114, E5504–E5512.

33. He, Y.; Galli, G. Perovskites for solar thermoelectric applications: A first principle study of CH3NH3AI3 (A = Pb and Sn). Chem. Mater. 2014, 26, 5394–5400.

34. Eom, J.H.; Choi, H.J.; Pammi, S.V.N.; Tran, V.D.; Kim, Y.J.; Kim, H.J.; Yoon, S.-G. Self-powered pressure and light sensitive bimodal sensors based on long-term stable piezo-photoelectric MAPbI3 thin films. J. Mater. Chem. C 2018, 6, 2786–2792.

35. Xu, Z.; Wu, C.; Zhu, Y.; Ju, S.; Ma, F.; Guo, T.; Li, F.; Kim, T.W. Bio-inspired smart electronic-skin based on inorganic perovskite nanoplates for application in photomemories and mechanoreceptors. Nanoscale 2021, 13, 253–260.

36. Ma, C.; Lo, M.F.; Lee, C.S. Stabilization of organometallic halide perovskite nanocrystals in aqueous solutions and their applications in copper ion detection. Chem. Commun. 2018, 54, 5784–5787.

37. Sasmal, S.; Sinha, A.; Donnadieu, B.; Pala, R.G.S.; Sivakumar, S.; Valiyaveettil, S. Volatility and chain length interplay of primary amines: Mechanistic investigation on the stability and reversibility of ammonia-responsive hybrid perovskites. ACS Appl. Mater. Interfaces 2018, 10, 6711–6718.

38. Huang, G.; Khan, A.A.; Rana, M.M.; Xu, C.; Xu, S.; Saritas, R.; Zhang, S.; Rahmand, E.; Turban, P.; Girard, S.; et al. Achieving ultrahigh piezoelectricity in organic−inorganic vacancy-ordered halide double perovskites for mechanical energy harvesting. ACS Energy Lett. 2021, 6, 16–23.

39. Jella, V.; Ippili, S.; Eom, J.H.; Kim, Y.J.; Kim, H.J.; Yoo, S.-G. A novel approach to ambient energy (thermoelectric, piezoelectric and solar-TPS) harvesting: Realization of a single structured TPS-fusion energy device using MAPbI3. Nano Energy 2018, 52, 11–21.